CHAPTER 9

Stratospheric Ozone in the 21st Century

D. W. WAUGH,*[a] V. EYRING[b] AND D. E. KINNISON[c]

[a] Department of Earth and Planetary Sciences, Johns Hopkins University, Baltimore, Maryland, USA; [b] Deutsches Zentrum für Luft- und Raumfahrt, Institut für Physik der Atmosphäre, Oberpfaffenhofen, Germany; [c] National Center for Atmospheric Research, Boulder, CO, USA

9.1 Introduction

The stratospheric ozone layer has been depleted by anthropogenic emissions of halogenated species over the last decades of the 20th century. Observations show that tropospheric halogen loading is now decreasing, which reflects the controls of ozone-depleting substances (ODSs) by the Montreal Protocol and its Amendments and Adjustments (see Chapter 2).[1,2] The total abundance of ODSs in the troposphere peaked around 1993 and has slowly declined since then. This slow decline is expected to continue over the 21st century (21C), and ODS are expected to be back to 1980 levels around 2040, and to around 1970 levels by the end of the century (see Chapter 2). Atmospheric concentrations of greenhouse gases (GHGs) have also increased and are expected to further increase in the future, with consequences for the ozone layer.[3] As a result of climate change, the ozone layer will not return to precisely its unperturbed state when the abundance of halogens returns to background levels. Furthermore, climate change complicates the attribution of ozone recovery to the decline of ODSs.

To project the future evolution of stratospheric ozone and attribute its change in response to the different forcings, numerical models are required that

Stratospheric Ozone Depletion and Climate Change
Edited by Rolf Müller

Published by the Royal Society of Chemistry, www.rsc.org

can adequately represent the chemistry and dynamics of the ozone layer, along with the energetics and natural variability of the atmosphere. The coupling of stratospheric chemistry with climate models has led to a new generation of models far more complex than those available when the Montreal Protocol was signed over 20 years ago. Such models, known as Chemistry-Climate Models (CCMs), are three-dimensional atmospheric circulation models with fully coupled chemistry, *i.e.* where chemical reactions drive changes in atmospheric composition which in turn change the atmospheric radiative balance and hence dynamics. CCMs are key tools for the detection, attribution and projection of the response of stratospheric ozone to ODSs and other factors, and allow questions about future stratospheric ozone and solar ultraviolet (UV) radiation levels to be studied. In particular, by including an explicit representation of tropospheric climate change, they make it possible to address the coupling between climate change and ozone depletion/recovery in a comprehensive manner.

Over the past decade there have been several international projects evaluating stratospheric CCMs, and related General Circulation Models (GCMs), most of which have been organized under the auspices of the WCRP's (World Climate Research Programme) SPARC (Stratospheric Processes and their Role in Climate) project. For example, the GCM-Reality Intercomparison Project (GRIPS) and the Chemistry-Climate Model Validation (CCMVal) Activity.[4,5] These multi-model projects have contributed directly to the assessment of CCMs during the preparation of the World Meteorological Organization/United Nations Environment Programme (WMO/UNEP) Scientific Assessments of Ozone Depletion.[5–10]

This chapter discusses projections of the evolution of stratospheric ozone during the 21st century. We first describe the CCMs and simulations that have been used in the last decade to project stratospheric ozone (Section 9.2). Section 9.3 briefly reviews the major factors that are affecting the ozone projections which are discussed in Section 9.4. The uncertainties and open questions in the evolution of ozone (O_3) in the 21C are discussed in Section 9.5, and a summary is in Section 9.6.

9.2 Models and Simulations

9.2.1 Chemistry-climate Models

CCMs consist of coupled modules that calculate the dynamical fields (temperatures and winds), radiation (heating and cooling rates), and chemistry, see Figure 9.1. At each time step, the simulated concentrations of the radiatively active gases are used in the calculations of the net heating rates so that a change in the abundance of radiatively active gases feeds back on atmospheric dynamics fields (*e.g.* winds and temperature). Similarly, changes in dynamics feed back on the chemical composition.

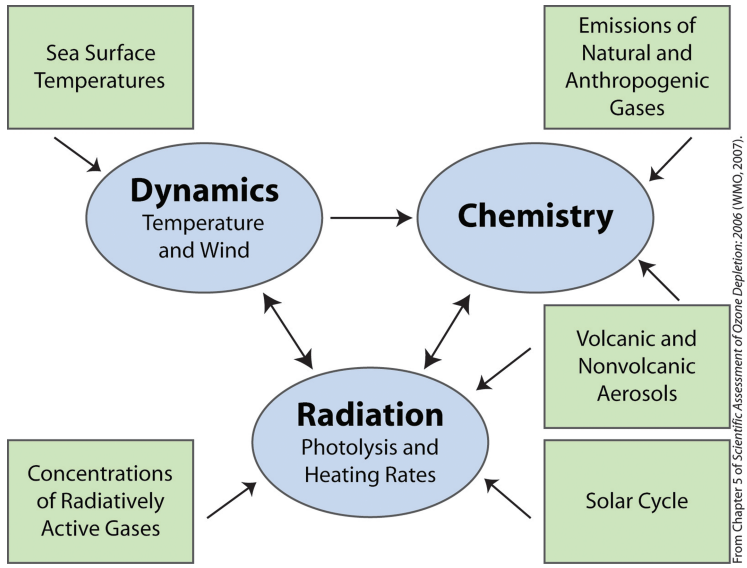

Figure 9.1 Schematic of a Chemistry-Climate Model (CCM). The core of a CCM (oval symbols) consists of a general circulation model (GCM) that includes calculation of the heating and cooling rates and a detailed chemistry module. They are interactively coupled. Photolysis rates are calculated online or are determined from a lookup table. Arrows indicate the direction of effect. Rectangular boxes denote external impacts. From Figure 5.1 of WMO (2007).[2]

The dynamics (*i.e.* the temporal evolution of wind, temperature and pressure, or other prognostic variables) in state-of-the-art CCMs is determined by solving the ''primitive'' equations. The basic dynamical state of the atmosphere within which transport takes place depends on a number of physical processes. These include the propagation of Rossby and gravity waves, wave-mean-flow interaction, and the diabatic circulation. Correct reproduction of the climatological mean state of the stratosphere by CCMs, including inter-hemispheric differences, inter-annual and intra-seasonal variability, is important but not sufficient: the basic dynamical mechanisms must be well represented in the underlying GCMs on which the CCMs are based if future changes are to be modeled credibly. A major issue with GCMs of the middle atmosphere is the treatment of gravity waves.[4] In addition, prescribed sea surface temperatures (SSTs) and sea ice concentrations (SICs) hinder the feedback between chemistry-climate interactions, so there is a need for a range of simulations looking at all aspects of the atmosphere-ocean system.

Radiative calculations are used in CCMs to derive photolysis rates and heating rates. Photolysis rates in the stratosphere affect the abundance of many chemical constituents that in turn control radiatively active constituents, such as O_3, nitrous oxide (N_2O), methane (CH_4), and chlorofluorocarbons (CFCs).

These radiatively active constituents are used in radiative heating calculations and therefore affect temperature and dynamics.

All CCMs used to make projections of ozone in the 21C include a comprehensive stratospheric chemistry scheme that is coupled to physical processes through the radiation calculations. This includes gas-phase and heterogeneous chemistry on aerosols and on polar stratospheric clouds (PSCs). One of the ways in which chemistry and dynamics are coupled is the temperature dependence of many chemical reaction rates. The importance of local control of ozone by chemistry relative to transport varies substantially between various times and places. In the upper stratosphere transport plays a role by controlling the concentrations of long-lived tracers such as inorganic chlorine, but photochemical timescales are so short that transport has a minimal direct impact on ozone. However, in the lower stratosphere, the photochemical timescales are longer (typically of the order of months) and interactions with dynamics are complex and more challenging to model accurately. In addition, aerosols and PSCs play an important role in chemistry of the lower stratosphere, since reactions can take place within or on the particles. In this region, heterogeneous reactions convert inorganic chlorine and bromine reservoir species to more active ozone-depleting species (Chapter 4). Consequently, even thought the photochemical lifetime of ozone is typically many months in the lower stratosphere, rapid chemical loss of ozone occurs when temperatures are cold, aerosols or PSCs exist, and sunlight is available (Chapter 5).

Transport in the stratosphere involves both meridional overturning (the so-called ''Brewer-Dobson'' circulation), and mixing. The most important aspects are the vertical (diabatic) mean motion and the horizontal mixing. Horizontal mixing is highly inhomogeneous, with transport barriers in the subtropics and at the edge of the wintertime polar vortex; mixing is most intense in the wintertime ''surf zone'', *i.e.* the region surrounding the polar vortex, and is comparatively weak in the summertime extratropics. Accurate representation of this structure in CCMs is important for the ozone distribution itself, as well as for the distribution of chemical families and species that affect ozone chemistry, *e.g.* Cl_y, total inorganic nitrogen (NO_y), total inorganic bromine (Br_y) water vapor (H_2O), and CH_4.

9.2.2 Simulations

CCMs have been used to perform several different types of simulations. Transient simulations consider observed or projected changes in concentrations of radiatively active gases and other boundary conditions (*e.g.*, emissions), whereas time-slice simulations are applied to study the internal variability of a CCM under fixed conditions, *e.g.*, GHG concentrations and SSTs, to estimate the significance of specific changes. Transient simulations are preferred for studying past and projecting future ozone changes because in these simulations, ozone responds interactively to the gradual secular trends in GHGs, ODSs, and other boundary conditions. The CCM simulations are commonly separated

into "past" (or "historical") transient simulations that are forced by observations of ODSs, GHGs, and SSTs, and are carried out to see how well the models can reproduce the past behavior of stratospheric ozone, and "future" transient simulations that are forced by trace gas projections and modeled SSTs and are carried out to make projections for the future evolution of stratospheric ozone. In addition, sensitivity or idealized simulations are performed where one or more of the forcing fields are held fixed or vary in an unrealistic manner to isolate the role of particular factors in driving changes in stratospheric O_3.

In recent years, the community has defined reference simulations, with a set of anthropogenic and natural forcings, to encourage consistency and comparison between simulations by different modeling groups.[11–13]

The *past reference simulation*, is defined as a transient run from 1960 to the present and is designed to reproduce the well-observed period of the last 30 years during which ozone depletion is well recorded.[14] This simulation examines the role of natural variability and other atmospheric changes important for ozone balance and trends. All forcings in this simulation are taken from observations. This transient simulation includes all anthropogenic and natural forcings based on changes in trace gases, solar variability, volcanic eruptions, quasi-biennial oscillation (QBO), and SSTs/SICs.[13]

The corresponding *future reference simulation* is a transient simulation from the past into the future (ideally 1960 to 2100), whose objective is to produce best estimates of future ozone-climate change up to 2100 under specific assumptions about GHG increases and decreases in halogen emissions in this period. GHG concentrations (N_2O, CH_4, and CO_2) in this reference simulation are prescribed following the Intergovernmental Panel on Climate Change Special Report on Emission Scenarios (IPCC SRES) "A1B" GHG scenario and surface mixing ratios of ODSs are based on the adjusted halogen scenario A1 from the 2006 WMO/UNEP Assessment, which includes the earlier phase-out of hydrochlorofluorocarbons (HCFCs) that was agreed to by the Parties to the Montreal Protocol in 2007, see Figure 9.2.[2,3] The future reference simulations typically include only anthropogenic forcings, and external natural forcings such as solar variability, and volcanic eruptions are not considered, as they cannot be known in advance.

The CCMVal reference simulations have been performed by most CCM groups in support of the 2006 and 2010 WMO/UNEP Assessments.[2,14] The first round of CCMVal (CCMVal-1) included 13 CCMs, whereas 18 CCMs participated in the most recent second round of CCMVal (CCMVal-2), see Table 9.1.[11] In addition, several different types of *sensitivity simulations* have been performed by a small subgroup of CCMs. For example, simulations with fixed halogens have been performed to study the effect of halogens on stratospheric ozone (and climate) in a changing climate' and "no greenhouse-gas induced climate change" simulations have been performed to address the coupling of ozone depletion/recovery and climate change.[15–17] The SRES A1B GHG scenario is only one of several scenarios for the possible evolution of GHGs, and future simulations have also been performed using a different GHG scenarios to assess the dependence of the future ozone evolution on the GHG scenario.[10,18]

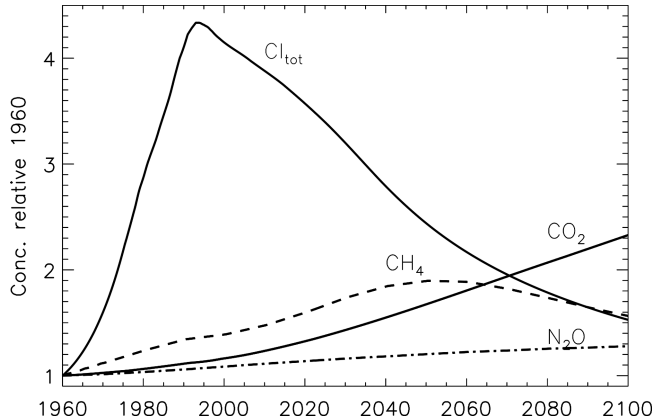

Figure 9.2 Time series of the surface concentrations of total chlorine from the WMO (2007) scenario, and GHGs from the IPCC SRES A1B scenario.[2,3] Concentrations are shown relative to their 1960 concentrations (820 ppt for Cl_{tot}, 1265 ppb for CH_4, 316 ppm for CO_2, and 291 ppb for N_2O).

Table 9.1 CCMs that are used for ozone projections in the CCMVal-2 intercomparison of SPARC CCMVal (2010): name of the model, group and references for model documentations.

	CCM	*Group and Location*	*References*
1	AMTRAC3	GFDL, USA	Austin and Wilson (2010)[46]
2	CAM3.5	NCAR, USA	Lamarque *et al.* (2008)[47]
3	CCSRNIES	NIES, Tokyo, Japan	Akiyoshi *et al.* (2009)[48]
4	CMAM	MSC, University of Toronto, York Univ., Canada	Scinocca *et al.* (2008);[49] deGrandpre *et al.* (2000)[50]
5	CNRM-ACM	Meteo-France; France	Déqué (2007);[51] Teyssèdre *et al.* (2007)[52]
6	E39CA	DLR, Germany	Stenke *et al.* (2009);[53] Garny *et al.* (2008)[54]
7	EMAC	MPI Mainz, Germany	Jöckel *et al.* (2006)[55]
8	GEOSCCM	NASA/GSFC, USA	Pawson *et al.* (2008)[56]
9	LMDZrepro	IPSL, France	Jourdain *et al.* (2008)[57]
10	MRI	MRI, Japan	Shibata and Deushi (2008a,b)[58,59]
11	NIWA-SOCOL	NIWA, NZ	Schraner *et al.* (2008);[60] Egorova *et al.* (2005)[61]
12	SOCOL	PMOD/WRC and ETHZ, Switzerland	Schraner *et al.* (2008);[60] Egorova *et al.* (2005)[61]
13	ULAQ	University of L'Aquila, Italy	Pitari *et al.* (2002);[62] Eyring *et al.* (2006; 2007)[8,9]
14	UMETRAC	NIWA, NZ	Austin and Butchart (2003)[63]
15	UMSLIMCAT	University of Leeds, UK	Tian and Chipperfield (2005);[64] Tian *et al.* (2006)[65]
16	UMUKCA-METO	MetOffice, UK	Morgenstern *et al.* (2008, 2009)[66,67]
17	UMUKCA-UCAM	University of Cambridge, UK	Morgenstern *et al.* (2008, 2009)[66,67]
18	WACCM	NCAR, USA	Garcia *et al.* (2007)[68]

9.2.3 Evaluation

Confidence in, and guidance in interpreting, CCM projections of future changes in atmospheric composition can be gained by first ensuring that the CCMs are able to reproduce past observations. Limitations and deficiencies in the models can be revealed through intermodel comparisons and through comparisons with observations. As well as evaluating the simulations of the state of the atmosphere, it is also important to evaluate the representation in the models of key processes that control the distribution of stratospheric ozone.[5] Also, with the increasing number of CCMs and the large spread in ozone projections, there is a need for multi-model comparison in addition to single model studies.

Over the last decade there have been several multi-model comparisons that have evaluated different aspects of the CCMs. Austin *et al.* evaluated a mixture of time-slice and transient simulations from eight CCMs.[6] They focused on diagnostics to evaluate the representation of dynamics in polar regions and found that many of the participating CCMs indicated a significant cold bias in high latitudes, the so-called "cold pole problem", particularly in the southern hemisphere during winter and spring. They concluded that the main uncertainties of CCMs at that time stemmed from the performance of the underlying GCM. Cold biases have been found to exist in the stratosphere in many CCMs, consistent with that previously found for models without chemistry.[4]

The 13 CCMs that participated in CCMVal-1 were evaluated and considered in the 2006 WMO/UNEP Assessment.[8,19] In contrast to previous studies, the CCM simulations were all transient simulations and had almost identical forcings (*e.g.*, SSTs, GHGs, and ODSs). This eliminated many of the uncertainties in the conclusions of the earlier assessments that resulted from the differences in experimental setup of individual models. Also, and perhaps most importantly, this study was the first multi-CCM assessment to evaluate the representation of transport and distributions of important trace gases. It was shown that there were substantial quantitative differences in the simulated stratospheric Cl_y, with the October mean Antarctic Cl_y peak value varying from less than 2 ppb to over 3.5 ppb in the participating CCMs. These large differences in Cl_y among the CCMs have been found to be key to diagnosing the intermodel differences in simulated ozone recovery, in particular in the Antarctic, (see further discussion below).[9] Several other studies evaluated and analyzed different aspects in the CCMVal-1 simulations. For example, Gettelman *et al.* showed that the CCMs were able to reproduce the basic structure of the Tropical Tropopause Layer (TTL) but differences were found in cold point tropopause temperatures trends.[20] Austin *et al.* found that the mean model response is about 2.5% in ozone and 0.8 K in temperature during a typical solar cycle, which is at the lower end of the observed ranges of peak responses.[21]

A much more extensive evaluation of CCMs was performed as part of the 2010 SPARC CCMVal Report.[11] This report analyzed simulations from the 18 CCMs that participated in CCMVal-2. All 13 CCMs in CCMVal-1 participated again, but partly with updated and improved or new model versions; in

addition five new models submitted output to the CCMVal archive.[8] The SPARC CCMVal report included evaluation of a much larger set of processes than in previous evaluations, with an evaluation of dynamical, radiative, chemical, and transport processes, as well as upper troposphere/lower stratosphere and stratosphere-troposphere coupling.[8] The report also included the application of observationally based performance metrics to quantify the ability of models to reproduce key processes. Overall, the performance of CCMVal-2 models is similar to those in CCMVal-1. There are some diagnostics for which there is improvement (*e.g.*, Cl_y) but for other diagnostics the general model performance is worse and the spread of models is larger (*e.g.*, 100 hPa temperature and water vapor).

9.3 Changes in Major Factors Affecting Stratospheric Ozone

As discussed in the Introduction, the increase in stratospheric chlorine and bromine over the last few decades was the dominant cause of decreases in O_3 over this period. However, as discussed in Chapter 8, climate change is likely to have an increasing role in O_3 changes over the next century. Therefore, before discussing the projected ozone evolution, we examine the changes in the factors that control the distribution of O_3 as projected in the CCM simulations.

9.3.1 Stratospheric Halogens

The abundance of surface total chlorine (Cl_{tot}) and total bromine (Br_{tot}) peaked around 1993 and has slowly declined since then (see Figure 9.3).[14] This slow decline is expected to continue over the 21C, and ODSs are expected to be back to 1980 levels in the 2030s and be below 1970 levels by the end of this century. The stratospheric chlorine and bromine loading is expected to evolve in a similar manner, although with a transport-related time delay. A commonly used variable for the effect of halogens on stratospheric ozone is the Effective Equivalent Stratospheric Chlorine (EESC).[22,23] The EESC is an empirical estimate of stratospheric reactive chlorine and bromine, based on measurements and projections of surface ODS, observational estimates of the transit times between the troposphere and stratosphere and the fractional release rates of different ODS. Fractional release is the fraction of inorganic halogen released from halocarbons at a given location and time. Calculations of EESC appropriate for mid-latitude lower stratosphere (mean age of air $\sim$3 years) indicate a return of EESC to 1980 values around 2040, while calculations for polar regions (mean age of air $\sim$5.5 years) show a later return dates around 2065. There is a $\sim$25 year difference in return dates for polar and mid-latitude EESC, even though there is only a $\sim$2.5 year difference in mean age, because of the rapid growth of EESC around 1980 and slow decay around 2050.

The CCMs simulate Cl_y and Br_y within the stratosphere, and these concentrations can be used, rather than EESC, to examine variations in halogen

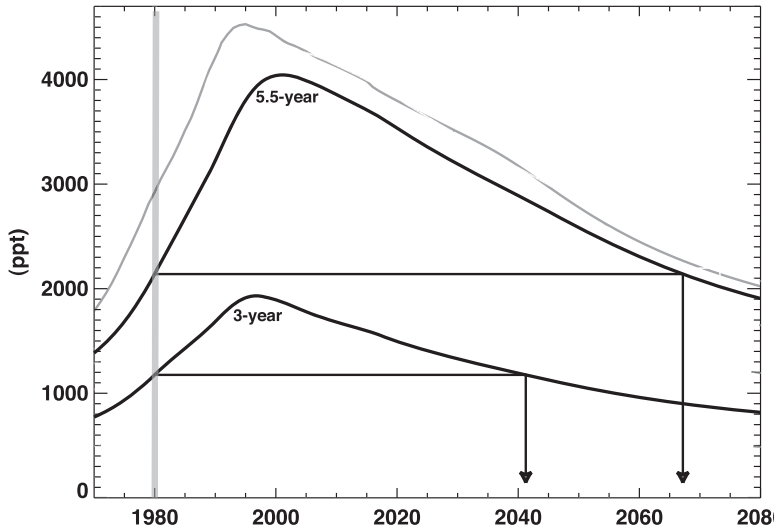

Figure 9.3 Evolution of surface $Cl_{tot} + 60Br_{tot}$ (gray curve) and EESC for mean age-of-air values of 3 and 5.5 years (black curves) for WMO (2002) ODS scenarios. The gray vertical line indicates the reference year of 1980. The black horizontal and vertical lines indicate the recovery date of EESC to 1980 values. From Figure 5 of Newman *et al.* (2007).[23]

that effect ozone (Chapter 2). As discussed in Section 9.2, the CCM simulations use a common scenario for the surface concentrations of ODSs when making projections. However, although the general evolution of Cl_y and Br_y is similar between CCMs, there are significant variations in the peak values of Cl_y and Br_y and the timing of the return to historical levels. For example, in the polar lower stratosphere, the simulated peak value of Cl_y in the individual CCMVal-2 models varies between 2.2 and 3.3 ppb, and the year when Cl_y returns to its 1980 value varies between 2040 and 2080 (see Figure 9.13 in the SPARC CCMVal report).[11] These two aspects are generally related, with CCMs with lower peak Cl_y values projecting an earlier return of Cl_y to pre-1980 values. The resulting evolution of Cl_y in the CCMVal-2 multi-model mean along with its uncertainty is shown in Figure 9.4.

As discussed in Section 9.2.3, the observed peak Cl_y in polar regions is around 3.3 ppb and most CCMs underestimate this peak value. This bias and the fact that models with lower peak return to 1980 values earlier needs to be considered when interpreting the CCM projections of ozone.

9.3.2 Temperature

As discussed in Chapter 8, changes in stratospheric temperatures can impact ozone loss by changing the rate of chemical reactions and the formation of PSCs. The stratosphere has cooled over the last four decades, and cooling is expected to continue through the 21C.[9,11,24] The cooling over the past few

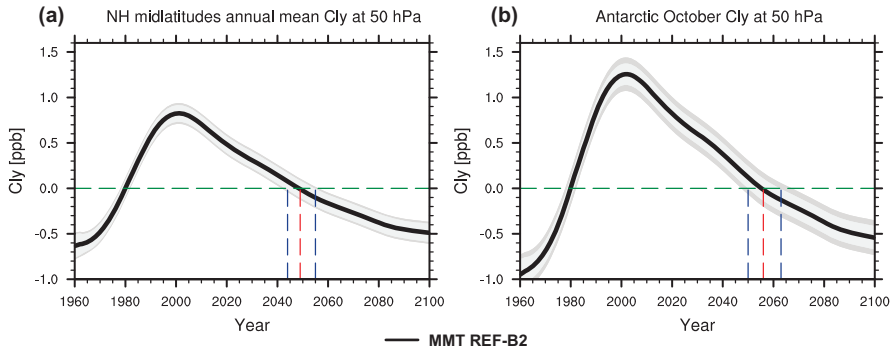

Figure 9.4 1980 baseline-adjusted multi-model trend estimates of annually averaged inorganic chlorine (Cl_y) at 50 hPa (ppb) for **(a)** annual northern midlatitude mean 35–60°N and **(b)** Antarctica (60°S–90°S) in October. The red vertical dashed line indicates the year when the multi-model trend in Cl_y returns to 1980 values and the blue vertical dashed lines indicate the uncertainty in these return dates. Multi-model mean derived from Figures 3.6 and 3.11 of WMO (2011).[14]

decades can be attributed to contributions from both increasing CO_2 and decreasing O_3 (the latter caused by increasing ODSs).[25,26] The impact of increasing CO_2 is expected to be dominant through the 21C, and CCMs show cooling in extra-polar regions throughout the 21C. The cooling rate increases with altitude, and the projected cooling in the upper stratosphere in the 21C is around 1 K/decade (Figure 9.5). This cooling in the middle and upper stratosphere will decrease the rate of the gas-phase chemical reactions that destroy O_3 (Chapter 1, 6), and cause O_3 to return to historical values earlier than expected just from changes in stratospheric halogens.

In the polar lower stratosphere, temperature trends could alter O_3 by a different mechanism; namely, a cooling could lead to increase in the temporal and spatial extent of PSCs. This would increase the occurrence of heterogeneous chemical reactions that lead to ozone depletion. There are large seasonal variations in polar temperature trends, but the winter/early spring trends are most relevant for understanding polar ozone depletion. CCM projections are not uniform on whether there is a cooling or warming in either polar region, but nearly all indicate that any trends will likely be small.[9,24] Understanding and quantifying trends in polar lower stratospheric temperatures during late winter/spring is complicated by the large year-to-year variability (especially in the northern hemisphere) which tends to interfere with any long-term trend detection. The lack of large winter trends could be due to increased downwelling and diabatic warming, compensating the radiative cooling due to increasing GHGs.

9.3.3 Transport

Another factor that could influence the 21C evolution of stratospheric O_3 is a change in stratospheric circulation. Changes in stratospheric dynamics alter the

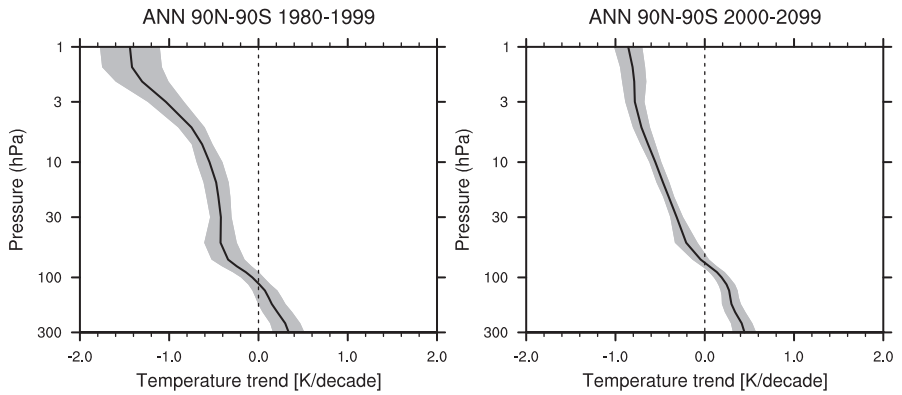

Figure 9.5 Multi-model annual mean 90°S–90°N temperature trend from 1980 to 1999 (left panel), and from 2000 to 2099 (right panel). The black line shows the CCMVal-2 multi-model mean and the shaded region shows ±1 standard deviation about the mean. Multi-model mean derived from Figure 4.4 of *SPARC CCMVal* (2010).[11]

stratospheric circulation, which then impacts the O_3 distribution by altering the direct transport of O_3 among regions, as well as by altering the distribution of Cl_y and Br_y, and other species involved in O_3 destruction. A robust result of modeling studies is that an increase in GHGs leads to an increase in the tropical vertical velocities (upwelling).[24,27,28] This is illustrated in Figure 9.6, which shows the multi-model mean and variance for projections of the tropical upwelling over the 21C. When GHGs and SSTs are increased, there is a significant increase in the upwelling ("REF"), whereas in a simulation with no climate change with GHG and SSTs fixed at 1960 levels, there is no change in the upwelling ("fGHG").[16] The increase in tropical upwelling leads to reduced transport time scales and a decrease in the mean age of air in the stratosphere.[24] The CCM simulations also indicate that there has been an increase in the tropical upwelling and a decrease in mean age of air over the past few decades.[17,29–31] However, this decrease has not been confirmed by observations, and a study by Engel *et al.* provided evidence that there has been a very small increase in the mean age of air over the last three decades.[32] There are, however, large uncertainties in the estimates of mean age from observations, and the cause of the discrepancy between the model and observations is unknown.[33,34]

The impact on O_3 of this acceleration of the stratospheric circulation will vary between regions. For example, an increase in upwelling will decrease tropical ozone below the peak in O_3 concentrations (below $\sim$10 hPa) but will increase tropical ozone above this peak. An increase in the meridional circulation will also likely increase O_3 in middle latitudes due to increased transport from tropical source region. We also expect the impact of changes in transport to be larger in the lower stratosphere, where photochemical timescales are longer, than in the upper stratosphere where ozone is under photochemical control.

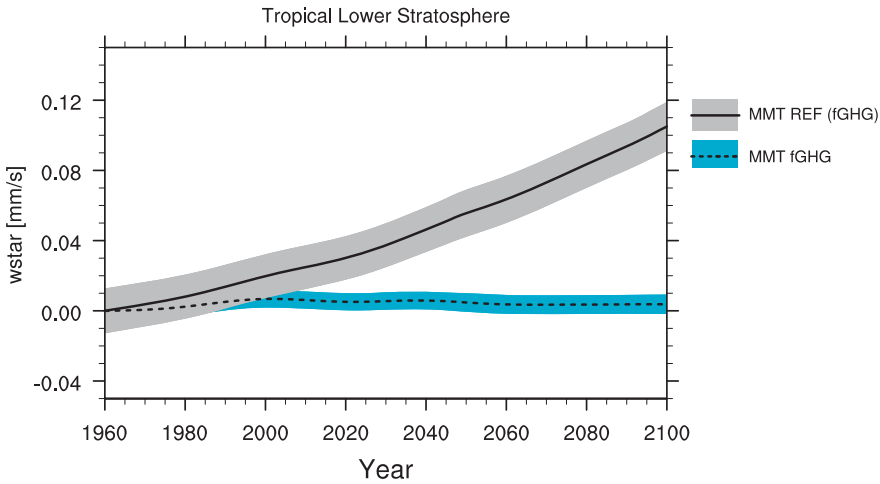

Figure 9.6 Multi-model mean and 95% confidence interval of the 1960 baseline-adjusted annual mean tropical upwelling mass flux between 20°S and 20°N at 70 hPa from the CCMVal-2 reference simulations (MMT REF, solid black line and grey shaded area) and the fixed greenhouse gas simulations (MMT fGHG, black dashed line and blue shaded area). From Figure 5 of Eyring *et al.* (2010).[16]

9.3.4 Other Factors

The long-term evolution of O_3 could also be altered by changes in nitrogen and hydrogen species that are involved in ozone destruction (see Chapter 8).

Increases in tropospheric N_2O are expected to occur in the 21C, leading to an increase in stratospheric NO_y. This would in turn be expected to lead to a decrease in ozone in the middle and upper stratosphere due to increased O_3 destruction by nitrogen oxides (NO_x). However, the percentage decrease in ozone is expected to be much smaller than the percentage N_2O increase. The increase in NO_y is smaller than N_2O due to temperature decreases in the upper stratosphere.[35] For example, the surface concentration of N_2O under scenario A1B increases by around 16% between 1980 and 2050, but the CCMs project that over the same period the stratospheric NO_y generally increases by around 10% or less.

Although the increase in NO_y is small over the 21C and not a dominant factor when GHGs follow the SRES A1B scenario, this is not the case for all IPCC scenarios.[3] For example, for the SRES A2 scenario there is a larger increase in N_2O, and changes related to NO_y make a significant contribution to changes in upper stratospheric O_3 (*e.g.*, in the GEOS CCM the decrease in O_3 at 3 hPa related to NO_y is $\sim 1/3$ the increase related to Cl_y decreases).[36]

The evolution of ozone in the 21C could also be affected by changes in stratospheric water vapor. An increase in water vapor would increase hydrogen oxide (HO_X), and lead to increased ozone loss in the extra-polar lower and upper stratosphere, where HO_X dominates ozone loss. In addition to changing

HO_X, an increase in water vapor would affect PSC formation and heterogeneous reactions in the CCMs, which could lead to increased springtime polar ozone loss (see Chapter 8).

There are two mechanisms that could cause long-term increases in stratospheric H_2O: (i) increases in CH_4, which will lead to an increase in H_2O, due to increased production from CH_4 oxidation, and (ii) a warming of the tropical cold-point temperature (which controls the stratospheric entry value of H_2O). Surface concentrations of CH_4 are projected to increase over 21C, although there are large variations between GHG scenarios. Most CCMs indicate a warming of the tropical tropopause in the future, which would cause an additional increase in stratospheric H_2O, by increasing the concentrations entering the stratosphere.[9] However, the increase in stratospheric H_2O due to the warming of tropical tropopause is generally smaller than contribution from a CH_4.[37] Overall, the stratospheric global-mean water vapor trends simulated by the CCMs are small (for the A1B scenario), and are not likely to be a major cause of changes in stratospheric O_3. This might change, however, if methane increases, for example to the melting of permafrost.

9.4 Projections of the Behavior of Ozone

The impact of the different climate factors discussed above on ozone varies between regions, both with latitude and altitude. As a consequence, the ozone evolution varies between regions. This is illustrated in Figure 9.7, which shows the multi-model mean change in O_3 between 2000 and 2100 from the CCMVal-2 models.[18]

9.4.1 Tropical Ozone

As shown in Figure 9.7a, the change in tropical ozone between 2000 and 2100 is very different above and below $\sim$15 hPa. In the upper stratosphere ozone is projected to increase, whereas a decrease is projected in lower stratospheric O_3.[9,16] This contrast is clearly seen in the solid black curves in Figure 9.8, which shows the multi-model mean evolution of (a) upper and (b) lower stratospheric O_3 from the CCMVal-2 reference simulations.[16]

The different evolution of ozone in the tropical upper and lower stratosphere is due to the different role of climate change (and the different role of the mechanisms discussed in Section 9.3) in the two regions. The increase in tropical upper stratosphere O_3 is due mainly to decreases in halogen levels, which reduces the O_3 loss due to catalytic chlorine and bromine reactions, and cooling due to increased GHGs, which slows the chemical reactions that destroy O_3, (see Section 9.3 and Chapter 1). These two mechanisms make roughly equal contributions to the O_3 increase over the 21C (for the A1B GHG scenario).[9,15,36,38] This can be seen in Figure 9.8a by comparing the dashed (orange) and dotted (blue) curves (shaded regions), which show the projected changes in O_3 due to climate change and ODSs, respectively. The change due to

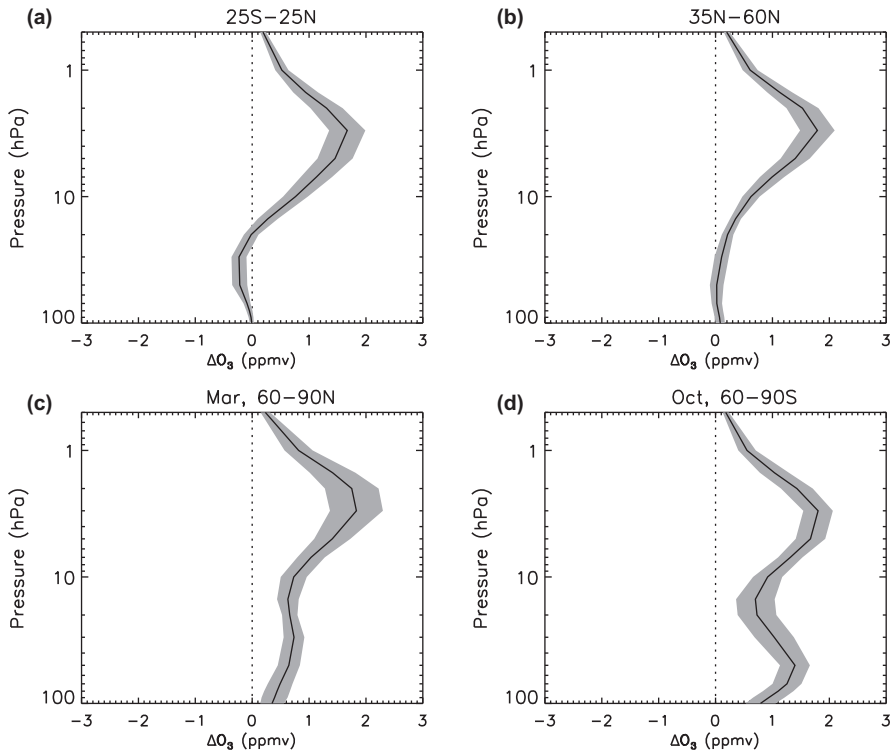

Figure 9.7 Multi-model mean of 2000–2100 ozone changes for different regions. The black line shows the CCMVal-2 multi-model mean and the shaded region shows ±1 standard deviation about the mean. Based on analysis in Oman *et al.* (2010).[18]

ODSs dominates over the latter part of the 20th century, but there is a similar increase in both terms over the 21C.

In the tropical lower stratosphere, the major mechanism causing long-term decreases in O_3 is the increase in tropical upwelling. As discussed in Section 9.3.3, a robust result in CCMs is an increase in tropical upwelling through the 21C. A future increase in upwelling in the tropics would result in a faster transit of air through the tropical lower stratosphere from an enhanced Brewer-Dobson circulation, which would lead to less time for production of ozone and hence lower ozone levels in this region.[14]

The fact that climate change is expected to increase O_3 in the tropical upper stratosphere, but to decrease O_3 in the tropical lower stratosphere means that if, and when, O_3 returns to historical values (*e.g.*, to values of O_3 in 1960 or 1980) varies between these altitudes. In the upper stratosphere, O_3 is projected to return to historical values several decades before upper stratospheric Cl_y and Br_y (and equivalent stratospheric chlorine, ESC; see Chapter 2) return to their historical values. For example, O_3 returns to 1960 values over 70 years before

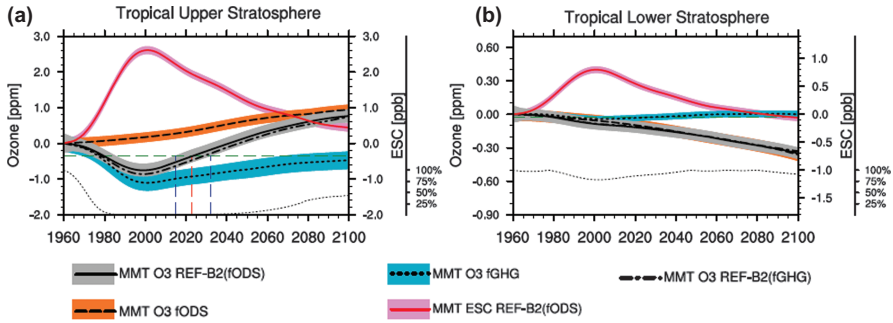

Figure 9.8 Tropical (25°S–25°N) annual mean 1960 baseline-adjusted ozone projections and 95% confidence for the (a) upper and (b) lower stratosphere. The multi-model trend (MMT) is shown for the CCMVal-2 reference run (REF-B2; black curves and grey shaded area), fixed ODS runs (fODS, black dotted line and orange shaded area), and fixed GHG runs (fGHG, black dashed line and blue shaded area). Also shown is the multi-model trend plus 95% confidence interval for Equivalent Stratospheric Chlorine (ESC), displayed with the red solid line and light red shaded area. See Figure 2 of Eyring *et al.* (2010a) for more details.[16]

Cl_y and Br_y return to their 1960 values (see Figure 9.8a). In the tropical lower stratosphere, O_3 may never return to historical values, even when anthropogenic ODSs have been removed from the atmosphere. For example, the multi-model mean O_3 decreases steadily from 1960 to 2100, even though Cl_y and Br_y return to 1960 values by the middle of the 21C, see Figure 9.8b.

The evolution of tropical column ozone depends on the balance between the increase in upper stratospheric concentrations and the decrease in lower stratospheric values, and as a result the projected changes are small, see Figure 9.9. There is no consensus between CCMs on whether tropical column ozone will return to pre-1980 values, with some models showing O_3 increasing slightly above 1980 values by the second half of the 21C, with O_3 remaining below 1980 values through the 21C. There is, however, a consensus that tropical column ozone will not return to 1960 values, *i.e.* even when stratospheric halogens return to historical (pre-1960) values, tropical column ozone will remain below its historical values.

9.4.2 Mid-latitude Ozone

The projected evolution of mid-latitude middle and upper stratosphere O_3 is very similar to that in the tropics (Figure 9.7b), with cooling in the upper stratosphere causing O_3 to return to historical values before Cl_y and Br_y. Furthermore, the magnitude of changes in O_3 and dates for returning to historical values are very similar to the tropics, as is the spread between CCMs. In the lower stratosphere, the evolution of mid-latitude O_3 differs somewhat from that in the tropics. In the subtropics O_3 decreases but at higher latitudes

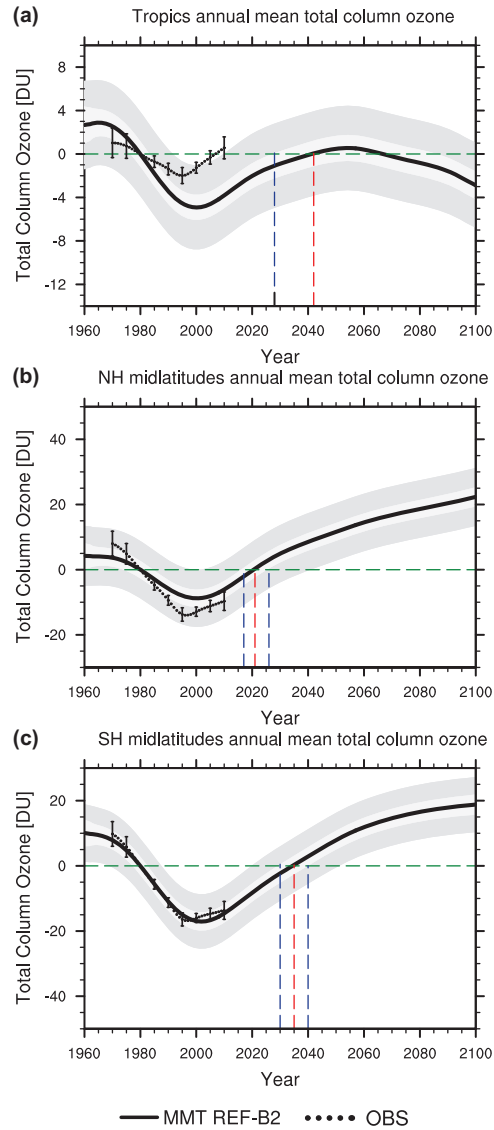

Figure 9.9 1980 baseline-adjusted multi-model trend estimates of annually averaged total column ozone (DU) for the tropics (25°S–25°N, upper panel) and mid-latitudes (middle panel: 35°N–60°N, lower panel: 35°S–60°S) (thick dark gray line) with 95% confidence and 95% prediction intervals appearing as light- and dark-gray shaded regions, respectively, about the trend (note the different vertical scale among the panels). The red vertical dashed line indicates the year when the multi-model trend in total column ozone returns to 1980 values and the blue vertical dashed lines indicate the uncertainty in these return dates. The black dotted lines show observed total column ozone, where a linear least squares regression model was used to remove the effects of the quasi-biennial oscillation, solar cycle, El Niño-Southern Oscillation, and volcanoes from four observational data sets. Multi-model mean derived from Figure 3.6 of WMO (2011).[14]

(and averaged over middle latitudes) there is an increase in lower stratospheric O_3. As in the tropics, changes in transport play an important role in these O_3 changes. However, in mid-latitudes the increase in the meridional circulation leads to an increase rather than a decrease in lower stratospheric O_3.[38,39]

Because ozone averaged over mid-latitudes increases in the upper and lower stratosphere over the 21C, a similar evolution is projected for mid-latitude total column ozone (see Figure 9.9). The evolution of mid-latitude column ozone is similar among the CCMs, with a broad minimum around 2000, which is followed by a slow increase back to and above 1980 values. In all CCMs, the return of O_3 to 1980 values occurs before that of Cl_y and Br_y. However, as can be seen by the multi-model mean standard deviation that is shown in Figure 9.9, there is a spread in the magnitude of the changes and time of return to 1980 values. This spread is closely linked to the spread in simulated Cl_y.[7,9]

In most CCMs there are interhemispheric differences in the evolution of column ozone. The qualitative evolution is the same but there is a difference in magnitude of anomalies and in the date of return to historical values. The anomalies are larger in the SH (because of spreading of ozone hole air into mid-latitudes) and the return of mid-latitude column O_3 to 1980 values occurs later in the SH. The difference in the date of return to 1980 values appears to be due to interhemispheric difference in changes in transport. The increase in stratospheric circulation driven by climate change transports more O_3 into NH mid-latitude lower stratosphere than SH.[38]

9.4.3 Springtime Polar Ozone

The largest ozone depletion is observed in the polar lower stratosphere during spring, especially in the Antarctic (see Chapter 5). As a result, a major focus of model simulations is the projected evolution of polar lower stratospheric ozone during spring.

Antarctic

All models project a qualitatively similar evolution for Antarctic (60 °–90 °S) ozone in spring, with a broad minimum around 2000, followed by a very slow increase and a return to 1980 values sometime around the middle of the century, see Figure 9.10b. There are, however, as in the extrapolar regions, significant quantitative differences among the models, including a wide spread in the minimum values around 2000 and dates when ozone returns to 1980 (or 1960) values.[7,9]

Several different ozone indices have been used to quantify variations in Antarctic ozone, including the polar cap average (Figure 9.10), ozone mass, daily minimum ozone, and area of the ozone hole (area of ozone less than 220 DU).[40] There are some differences in the evolution of these different diagnostics, in particular over the 2000 to 2030 period, where the rate of change varies. However, all diagnostics show the same broad evolution with a return to 1980 values around the middle of century, and a wide spread among the models in quantitative details.

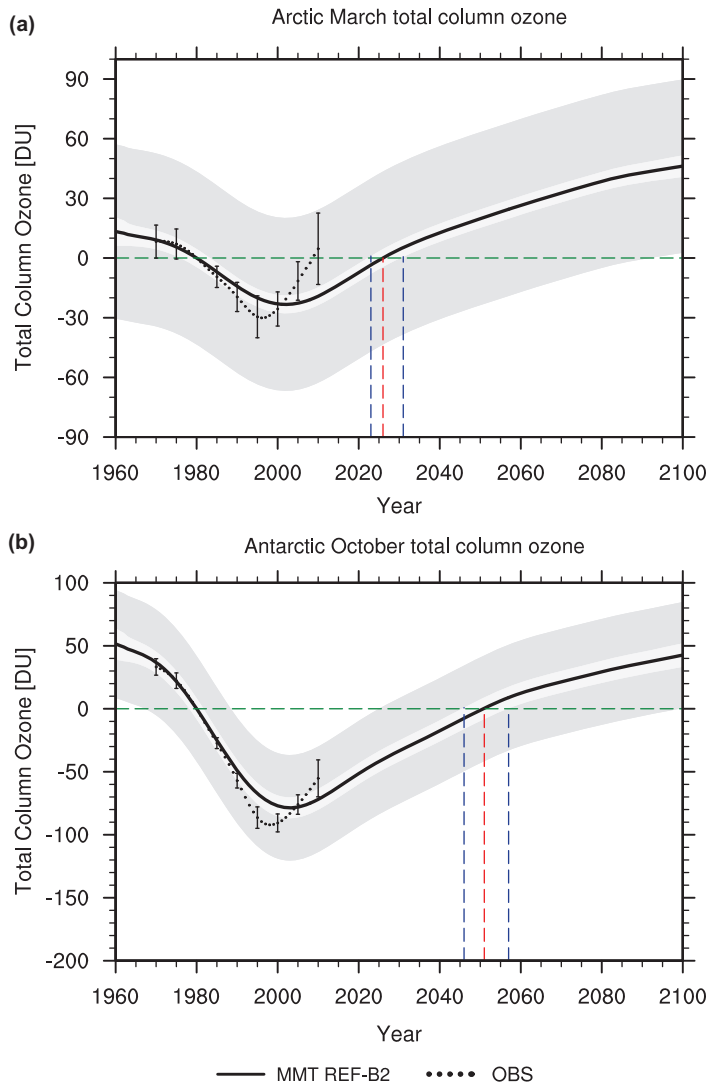

Figure 9.10 As in Figure 9.9, but for the latitude range 60°N–90°N in March (upper row) and the latitude range 60°S–90°S in October (lower row). The red vertical dashed line indicates the year when CCMVal-2 multi-model trend in total column ozone (DU) returns to 1980 values and the blue vertical dashed lines indicate the uncertainty in these return dates. Note the different vertical scale among the panels. Multi-model mean derived from Figure 3.10 of WMO (2011).[14]

The evolution of Antarctic spring ozone is dominated by the changes in Cl_y and Br_y, and changes in climate (temperature and transport) are not, in general, a major factor. This can be seen by the very close correspondence of the evolution of ozone and Cl_y (or ESC),[7,9,16] The spread in Antarctic ozone

projections are, as a result, primarily due to differences in simulated Cl_y (and Br_y) among the models. Models that simulate a smaller peak Cl_y have an earlier return of Cl_y to 1980 values, and generally also have smaller ozone depletion and earlier return of ozone to 1980 values. This relationship suggests that the low bias in Cl_y in most models results in an early bias in the projected return of ozone to 1980 values, *i.e.*, the return to 1980 values will likely occur later than indicated by the multi-model mean shown in Figure 9.10b.

Projections of the recovery of the Antarctic ozone hole have also been made using parametric models based on estimates of EESC and analyzed polar temperatures.[41] These calculations indicate that the ozone hole area will remain constant until around 2015, and then decrease to zero around 2070. This recovery date is later than that simulated by most models (see Figure 9b of Eyring *et al.* (2007)), but this difference is consistent with a bias in the models dynamics and transport.[9]

Arctic

Dynamical effects play a much larger role in the evolution of springtime Arctic ozone than in the Antarctic, and as a consequence there is large interannual variability. This interannual variability is much larger than the long-term changes, and time series need to be filtered (smoothed) to see long-term trends. However, long-term evolution of the filtered Arctic ozone is qualitatively the same as in other regions: there is a broad minimum around 2000 with slow increase over the first half of the 21C, see Figure 9.10a.

Although there is qualitative agreement among the models, there are large quantitative variations in the simulated changes in Arctic ozone, with some models showing only a small or even no change in ozone, while others show a large response to changes in halogens. There are substantial variations among the models in the date when ozone returns 1980 values (2020 to 2060), *e.g.*, see Figure 16 of Austin *et al.* (2010).[7]

An early study by Shindell *et al.* projected a substantial increase in Arctic ozone depletion, and the development of an Arctic ozone hole, because of climate change.[42] However, subsequent studies have not reproduced this result. Even though there is a large spread among the CCMs, in both CCMVal-1 and CCMVal-2, none of the CCMs predict large Arctic ozone decreases in the future.

Models project that Arctic ozone will return to 1980 values before Antarctic ozone, with the difference varying from only a few years in some models to over 25 years in others. The evolution of Cl_y and Br_y is similar in both polar regions, but because changes in temperature and transport play a significant role in the Arctic, the evolution of Arctic O_3 does not follow that of Cl_y and Br_y as closely as Antarctic ozone. In particular, acceleration of the Brewer-Dobson circulation and increases in polar temperatures cause an earlier return than that expected just because of changes in halogens.[43] These dynamical changes vary substantially among models, and as a consequence so do the differences in return dates of Arctic and Antarctic ozone.

9.5 Summary and Concluding Remarks

The evolution of stratospheric ozone in the 21st century will depend not only on changes (expected decreases) in the abundance of stratospheric halogens but also on changes due to increases in well-mixed greenhouse gases. The latter will cool the stratosphere, increase the abundance of nitrogen and hydrogen species involved in ozone destruction, and alter transport within the stratosphere. The impact of the greenhouse-gas-induced change on ozone varies between regions, and as a consequence the ozone evolution will vary between regions.

In the upper stratosphere the projected ozone evolution is very similar in the tropics and middle latitudes, with ozone increasing back to 1960 values in the first 2–3 decades of the 21st century. This rapid increase in ozone is due to both decreases in ODSs and cooling due to increased GHGs. The evolution in the mid-latitude lower stratosphere is similar to that in the upper stratosphere, although climate-change induced increases in the circulation play more of a role than cooling. In the tropical lower stratosphere the evolution is, however, very different: here ozone decreases throughout the 21st century due to climate-change-induced increases in the tropical upwelling. In the Antarctic, the models consistently show a broad minimum near year 2000 followed by a slower return to 1980 values than in middle latitudes (with the return delayed until the middle of the century). In the Arctic, the interannual variability in ozone is larger than long-term trends and the models are less consistent in their representation of ozone recovery. However, in most models Arctic ozone returns to 1980 values before Antarctic ozone.

Although there is generally qualitative agreement among models in the evolution of ozone, there are some substantial quantitative differences. In particular, there is a wide spread in projected ozone values at specified periods and in the dates when ozone returns to historical values. In many cases, the differences among model projections can be related to differences in the simulated Cl_y, and improving the transport of Cl_y, which will reduce the uncertainty in ozone projections, is a remaining major challenge.

It is also important to note that the ozone projections depend on scenarios for surface concentrations of ODSs and GHGs, and the majority of the projections have considered very similar ODS scenarios and the same GHG scenario. However, a recent examination of CCM projections for six different GHG scenarios found that lower GHG emissions result in: (i) smaller reductions in ozone in the tropical lower stratosphere (due to smaller increases in tropical upwelling), and (ii) smaller increases in upper stratospheric ozone globally (due to less severe stratospheric cooling).[10] Largest differences among the six GHG scenarios were found over northern mid-latitudes ($\sim$20 DU by 2100) and in the Arctic ($\sim$40 DU by 2100) with divergence mainly in the second half of the 21st century. The results suggest that effects of GHG emissions on future stratospheric ozone should be considered in climate change mitigation policy and ozone projections should be assessed under more than a single GHG scenario.

Future assessments should also consider the uncertainty in how the models force the organic halogen lower boundary condition. Currently, projections of future organic halogen loadings are based on projected emission rates and an estimate of the global atmospheric lifetime of each organic halogen. These factors are then used to create time-dependent volume mixing ratio lower boundary conditions, that are then used to force the CCMs. However, the destruction of each halogen in the CCMs is dependent on the tropical upwelling, meridional mixing, and chemical loss rates (*e.g.*, photolysis rates), and the CCM-derived halogen lifetimes can be very different from the lifetimes assumed for the given projection scenario. By forcing all CCMs to use fixed mixing ratio lower boundary conditions, the flux into the tropical lower stratosphere is fixed in all the models. This minimizes the spread in model-derived ozone return dates.[44] If models were forced with flux lower boundary conditions, the simulated ODS would be consistent with the simulated loss of ODSs and any changes in the model circulation would also feedback on these loss rates. Models with a more realistic circulation (*e.g.*, representation of mean age) would also more accurately represent the fractional release of inorganic halogens from their parent organic. This approach would give a more accurate representation of ozone depletion and recovery.

Another consideration for future simulations is inclusion of interactive ocean and sea ice modules in the CCMs. In all but one of the CCM simulations discussed above, the sea surface temperatures and sea ice concentrations were prescribed, and the important coupling between the atmosphere and oceans/cyrosphere are not represented. The one exception is the Canadian Middle Atmosphere Model (CMAM), in which the atmospheric model is coupled to an ocean/sea ice model.[45] Inclusion of these couplings in the CCMs leads to a more complete representation of the climate system and feedbacks, which could be particularly important for simulations of stratospheric polar ozone and its impact on tropospheric climate.

Acknowledgements

We acknowledge the Chemistry-Climate Model Validation (CCMVal) Activity of the World Climate Research Programme's (WCRP) Stratospheric Processes and their Role in Climate (SPARC) project for organizing and coordinating the model data analysis, and the British Atmospheric Data Centre (BADC) for collecting and archiving the CCMVal model output. We thank Anne Douglass for a careful review of this chapter and Irene Cionni and Luke Oman for preparing some of the figures. This research was supported by the US National Science Foundation and by the German Aerospace Center (DLR).

References

1. S. A. Montzka, J. H. Butler, B. D. Hall, D. J. Mondeel and J. W. Elkins, *Geophys. Res. Lett.*, **30**, 1826, doi:10.1029/2003GL017745, 2003.

2. World Meteorological Organization (WMO)/United Nations Environment Programme (UNEP), Scientific Assessment of Ozone Depletion: 2006, World Meteorological Organization, Global Ozone Research and Monitoring Project, Report No. 50, Geneva, Switzerland, 2007.
3. Intergovernmental Panel on Climate Change (IPCC) (2000), *Special Report on Emissions Scenarios: A Special Report of Working Group III of the Intergovernmental Panel on Climate Change*, 599 pp., Cambridge Univ. Press, Cambridge, U. K.
4. S. Pawson, K. Kodera, K. Hamilton, T. G. Shepherd, S. R. Beagley, B. A. Boville, J. D. Farrara, T. D. A. Fairlie, A. Kitoh, W. A. Lahoz, U. Langematz, E. Manzini, D. H. Rind, A. A. Scaife, K. Shibata, P. Simon, R. Swinbank, L. Takacs, R. J. Wilson, J. A. Al-Saadi, M. Amodei, M. Chiba, L. Coy, J. de Grandpré, R. S. Eckman, M. Fiorino, W. L. Grose, H. Koide, J. N. Koshyk, D. Li, J. Lerner, J. D. Mahlman, N. A. McFarlane, C. R. Mechoso, A. Molod, A. O'Neill, R. B. Pierce, W. J. Randel, R. B. Rood and F. Wu, *Bull. Am. Meteorol. Soc.*, 2000, **81**, 781–796.
5. V. Eyring, N. R. P. Harris, M. Rex, T. G. Shepherd, D. W. Fahey, G. T. Amanatidis, J. Austin, M. P. Chipperfield, M. Dameris, P. M. De, F. Forster, A. Gettelman, H. F. Graf, T. Nagashima, P. A. Newman, S. Pawson, M. J. Prather, J. A. Pyle, R. J. Salawitch, B. D. Santer and D. W. Waugh, *Bull. Am. Meteorol. Soc.*, 2005a, **86**, 1117–1133.
6. J. Austin, D. Shindell, S. R. Beagley, C. Brühl, M. Dameris, E. Manzini, T. Nagashima, P. Newman, S. Pawson, G. Pitari, E. Rozanov, C. Schnadt and T. G. Shepherd, *Atmos. Chem. Phys.*, 2003, **3**, 1–27.
7. J. Austin, J. Scinocca, D. Plummer, L. Oman, D. Waugh, H. Akiyoshi, S. Bekki, P. Braesicke, N. Butchart, M. P. Chipperfield, D. Cugnet, M. Dameris, S. Dhomse, V. Eyring, S. Frith, R. Garcia, H. Garny, A. Gettelman, S. C. Hardiman, D. Kinnison, J. F. Lamarque, E. Mancini, M. Marchand, M. Michou, O. Morgenstern, T. Nakamura, S. Pawson, G. Pitari, J. Pyle, E. Rozanov, T. G. Shepherd, K. Shibata, H. Teyssedre, R. J. Wilson and Y. Yamashita, *J. Geophys. Res.*, doi:10.1029/2010JD013857, 2010.
8. V. Eyring, N. Butchart, D. W. Waugh, H. Akiyoshi, J. Austin, S. Bekki, G. E. Bodeker, B. A. Boville, C. Brühl, M. P. Chipperfield, E. Cordero, M. Dameris, M. Deushi, V. E. Fioletov, S. M. Frith, R. R. Garcia, A. Gettelman, M. A. Giorgetta, V. Grewe, L. Jourdain, D. E. Kinnison, E. Mancini, E. Manzini, M. Marchand, D. R. Marsh, T. Nagashima, P. A. Newman, J. E. Nielsen, S. Pawson, G. Pitari, D. A. Plummer, E. Rozanov, M. Schraner, T. G. Shepherd, K. Shibata, R. S. Stolarski, H. Struthers, W. Tian and M. Yoshiki, *J. Geophys. Res.*, **111**, D22308, doi:10.1029/2006JD007327, 2006.
9. V. Eyring, D. W. Waugh, G. E. Bodeker, E. Cordero, H. Akiyoshi, J. Austin, S. R. Beagley, B. Boville, P. Braesicke, C. Brühl, N. Butchart, M. P. Chipperfield, M. Dameris, R. Deckert, M. Deushi, S. M. Frith, R. R. Garcia, A. Gettelman, M. Giorgetta, D. E. Kinnison, E. Mancini,

E. Manzini, D. R. Marsh, S. Matthes, T. Nagashima, P. A. Newman, J. E. Nielsen, S. Pawson, G. Pitari, D. A. Plummer, E. Rozanov, M. Schraner, J. F. Scinocca, K. Semeniuk, T. G. Shepherd, K. Shibata, B. Steil, R. Stolarski, W. Tian and M. Yoshiki, *J. Geophys. Res.*, 112, D16303, doi:10.1029/2006JD008332, 2007.

10. V. Eyring, I. Cionni, J. F. Lamarque, H. Akiyoshi, G. E. Bodeker, A. J. Charlton-Perez, S. M. Frith, A. Gettelman, D. E. Kinnison, T. Nakamura, L. D. Oman, S. Pawson and Y. Yamashita, *Geophys. Res. Lett.*, **37**, L16807, doi:10.1029/2010GL044443, 2010.
11. SPARC CCMVal (2010), SPARC Report on the Evaluation of Chemistry-Climate Models, V. Eyring, T. G. Shepherd, D. W. Waugh (Eds.), SPARC Report No. 5, WCRP-132, WMO/TD-No. 1526, http://www.atmosp.physics.utoronto.ca/SPARC.
12. V. Eyring, D. E. Kinnison and T. G. Shepherd, *SPARC Newsletter No. 25*, 2005b, 11–17.
13. V. Eyring, M. P. Chipperfield, M. A. Giorgetta, D. E. Kinnison, E. Manzini, K. Matthes, P. A. Newman, S. Pawson, T. G. Shepherd and D. W. Waugh, *SPARC Newsletter No. 30*, p. 20–26, 2008.
14. World Meteorological Organization (WMO)/United Nations Environment Programme (UNEP), Scientific Assessment of Ozone Depletion: 2010, World Meteorological Organization, Global Ozone Research and Monitoring Project, Report No. 52, Geneva, Switzerland, 2011.
15. D. W. Waugh, L. Oman, S. R. Kawa, R. S. Stolarski, S. Pawson, A. R. Douglass, P. A. Newman and J. E. Nielsen, *Geophys. Res. Lett.*, **36**, L03805, doi:10.1029/2008GL036223, 2009.
16. V. Eyring, I. Cionni, G. E. Bodeker, A. J. Charlton-Perez, D. E. Kinnison, J. F. Scinocca, D. W. Waugh, H. Akiyoshi, S. Bekki, M. P. Chipperfield, M. Dameris, S. Dhomse, S. M. Frith, H. Garny, A. Gettelman, A. Kubin, U. Langematz, E. Mancini, M. Marchand, T. Nakamura, L. D. Oman, S. Pawson, G. Pitari, D. A. Plummer, E. Rozanov, T. G. Shepherd, K. Shibata, W. Tian, P. Braesicke, S. C. Hardiman, J. F. Lamarque, O. Morgenstern, D. Smale, J. A. Pyle and Y. Yamashita, *Atmos. Chem. Phys.*, **10**, 9451-9472, doi:10.5194/acp-10-9451-2010, 2010.
17. R. R. Garcia and W. J. Randel, *J. Atmos. Sci.*, 2008, **65**, 2731–2739.
18. L. D. Oman, D. A. Plummer, D. W. Waugh, J. Austin, J. F. Scinocca, A. R. Douglass, R. J. Salawitch, T. Canty, H. Akiyoshi, S. Bekki, P. Braesicke, N. Butchart, M. P. Chipperfield, D. Cugnet, S. Dhomse, V. Eyring, S. Frith, S. C. Hardiman, D. E. Kinnison, J.-F. Lamarque, E. Mancini, M. Marchand, M. Michou, O. Morgenstern, T. Nakamura, J. E. Nielsen, D. Olivie, G. Pitari, J. Pyle, E. Rozanov, T. G. Shepherd, K. Shibata, R. S. Stolarski, H. Teyssedre, W. Tian, Y. Yamashita and J. R. Ziemke, *J. Geophys. Res.*, **115**, D24306, doi:10.1029/2010JD014362, 2010.
19. D. W. Waugh and V. Eyring, *Atmos. Chem. Phys.*, 2008, **8**, 5699–5713.
20. A. Gettelman, T. Birner, V. Eyring, H. Akiyoshi, S. Bekki, C. Brühl, M. Dameris, D. E. Kinnison, F. Lefevre, F. Lott, E. Mancini, G. Pitari,

D. A. Plummer, E. Rozanov, K. Shibata, A. Stenke, H. Struthers and W. Tian, *Atmos. Chem. Phys.*, 2009, **9**, 1621–1637.
21. J. Austin, K. Tourpali, E. Rozanov, H. Akiyoshi, S. Bekki, G. Bodeker, C. Brühl, N. Butchart, M. Chipperfield, M. Deushi, V. I. Fomichev, M. A. Giorgetta, L. Gray, K. Kodera, F. Lott, E. Manzini, D. Marsh, K. Matthes, T. Nagashima, K. Shibata, R. S. Stolarski, H. Struthers and W. Tian, *J. Geophys. Res.*, 2008, **113**, D11306.
22. J. S. Daniel, S. Solomon, R. W. Portmann and R. R. Garcia, *J. Geophys. Res.*, 1999, **104**, 23,871-23,880.
23. P. A. Newman, J. S. Daniel, D. W. Waugh and E. R. Nash, *Atmos. Chem. Phys.*, 2007, **7**, 4537–4552.
24. N. Butchart, I. Cionni, V. Eyring, T. G. Shepherd, D. W. Waugh, H. Akiyoshi, J. Austin, C. Bruhl, M. P. Chipperfield, E. Cordero, M. Dameris, R. Deckert, S. Dhomse, S. M. Frith, R. R. Garcia, A. Gettelman, M. A. Giorgetta, D. E. Kinnison, F. Li, E. Mancini, C. McLandress, S. Pawson, G. Pitari, D. A. Plummer, E. Rozanov, F. Sassi, J. F. Scinocca, K. Shibata, B. Steil and W. Tian, *J. Climate*, **23**, 5349–5374, doi: 10.1175/2010JCLI3404.1, 2010.
25. T. G. Shepherd and A. I. Jonsson, *Atmos. Chem. Phys.*, 2008, **8**, 1435–1444.
26. R. S. Stolarski, A. R. Douglass, P. A. Newman, S. Pawson and M. R. Schoeberl, *J. Climate*, 2010, **23**, 28–42.
27. N. Butchart, A. A. Scaife, M. Bourqui, J. de Grandpré, S. H. E. Hare, J. Kettleborough, U. Langematz, E. Manzini, F. Sassi, K. Shibata, D. Shindell and M. Sigmond, *Clim. Dyn.*, 2006, **27**, 727–741.
28. N. Butchart and A. A. Scaife, *Nature*, 2001, **410**, 799–802.
29. J. Austin, J. Wilson, F. Li and H. Vomel, *J. Atmos. Sci.*, 2007, **64**, 905–921.
30. L. Oman, D. W. Waugh, S. Pawson, R. S. Stolarski and P. A. Newman, *J. Geophys. Res.*, **114**, D03105, doi:10.1029/2008JD010378, 2009.
31. C. McLandress and T. G. Shepherd, *J. Clim*, 2009, **22**, 1516–1540.
32. A. Engel, T. Möbius, H. Bönisch, U. Schmidt, R. Heinz, I. Levin, E. Atlas, S. Aoki, T. Nakazawa, S. Sugawara, F. Moore, D. Hurst, J. Elkins, S. Schauffler, A. Andrews and K. Boering, *Nature Geosciences*, **2**, 28–31, 2009.
33. D. W. Waugh, *Nature Geosciences*, 2009, **2**, 14–16.
34. R. R. Garcia, W. J. Randel and D. E. Kinnison, *J. Atm. Sci.*, 2011, **68**, 139–154.
35. J. E. Rosenfield and A. R. Douglass, *Geophys. Res. Lett.*, 1998, **25**, 4381–4384.
36. L. Oman, D. W. Waugh, S. R. Kawa, R. S. Stolarski, A. R. Douglass and P. A. Newman, *J. Geophys. Res.*, **115**, D05303, doi:10.1029/2009JD012397, 2010.
37. L. Oman, D. W. Waugh, S. Pawson, R. S. Stolarski and J. E. Nielsen, *J. Atmos. Sci.*, 2008, **65**, 3278–3291.
38. T. G. Shepherd, *Atmos. Ocean*, 2008, **46**, 117–138.
39. F. Li, R. S. Stolarski and P. A. Newman, *Atmos. Chem. Phys.*, 2009, **9**, 2207–2213.

40. G. E. Bodeker, H. Shiona and H. Eskes, *Atmos. Chem. Phys.*, 2005, **5**, 2603–2615.
41. P. A. Newman, E. R. Nash, S. R. Kawa, S. A. Montzka and S. M. Schauffler, *Geophys. Res. Lett.*, **33**, L12814, doi:10.1029/2005GL025232, 2006.
42. D. T. Shindell, D. Rind and P. Lonergan, *Nature*, 1998, **392**, 589–592.
43. J. Austin and F. Li, *Geophys. Res. Lett.*, **33**, L17807, doi:10.1029/2006GL026867, 2006.
44. A. R. Douglass, R. S. Stolarski, M. R. Schoeberl, C. H. Jackman, M. L. Gupta, P. A. Newman, J. E. Nielsen and E. L. Fleming, *J. Geophys. Res.*, **113**, D14309, doi:10.1029/2007JD009575, 2008.
45. C. McLandress, A. I. Jonsson, D. A. Plummer, M. C. Reader, J. F. Scinocca and T. G. Shepherd, *J. Climate*, **23**, 5002–5020, doi: 10.1175/2010JCLI3586.1, 2010.
46. J. Austin and R. J. Wilson, *J. Geophys. Res.*, **115**, D18303, doi:10.1029/2009JD013292, 2010.
47. J.-F. Lamarque, D. E. Kinnison, P. G. Hess and F. M. Vitt, *J. Geophys. Res.*, **113**, D12301, doi:10.1029/2007JD009277, 2008.
48. H. Akiyoshi, L. B. Zhou, Y. Yamashita, K. Sakamoto, M. Yoshiki, T. Nagashima, M. Takahashi, J. Kurokawa, M. Takigawa and T. Imamura, *J. Geophys. Res.*, **114**, D03103, doi:10.1029/2007JD009261, 2009.
49. J. F. Scinocca, N. A. McFarlane, M. Lazare, J. Li and D. Plummer, *Atmos. Chem. Phys.*, 2008, **8**, 7055–7074.
50. J. de Grandpre, S. R. Beagley, V. I. Fomichev, E. Griffioen, J. C. McConnell, A. S. Medvedev and T. G. Shepherd, *J. Geophys. Res.*, 2000, **105**, 26475–26491.
51. M. Déqué, *Global and Planetary Change*, 2007, **57**, 16–26.
52. H. Teyssèdre, M. Michou, H. L. Clark, B. Josse, F. Karcher, D. Olivie, V.-H. Peuch, D. Saint-Martin, D. Cariolle, J.-L. Attié, P. Nédélec, P. Ricaud, V. Thouret, R. J. van der A, A. Volz-Thomas and F. Cheroux, *Atmos. Chem. Phys.*, 2007, **7**, 5815–5860.
53. A. Stenke, M. Dameris, V. Grewe and H. Garny, *Atmos. Chem. Phys.*, 2009, **9**, 5489–5504.
54. H. Garny, M. Dameris and A. Stenke, *Atmos. Chem. Phys.*, 2009, **9**, 6017–6031.
55. P. Jöckel, H. Tost, A. Pozzer, C. Brühl, J. Buchholz, L. Ganzeveld, P. Hoor, A. Kerkweg, M. G. Lawrence, R. Sander, B. Steil, G. Stiller, M. Tanarhte, D. Taraborrelli, J. van Aardenne and J. Lelieveld, *Atmos. Chem. Phys.*, 2006, **6**, 5067–5104.
56. S. Pawson, R. S. Stolarski, A. R. Douglass, P. A. Newman, J. E. Nielsen, S. M. Frith and M. L. Gupta, *J. Geophys. Res.*, **113**, D12103, doi:10.1029/2007JD009511, 2008.
57. L. Jourdain, S. Bekki, F. Lott and F. Lefèvre, *Annales Geophysicae*, 2008, **26**, 1391–1413.
58. K. Shibata and M. Deushi, *Annales Geophysicae*, 2008, **26**, 1299–1326.

59. K. Shibata and M. Deushi, Simulation of the stratospheric circulation and ozone during the recent past (1980–2004) with the MRI chemistry-climate model, CGER's Supercomputer Monograph Report Vol. 13, National Institute for Environmental Studies, Japan, 154 pp, 2008.
60. M. Schraner, E. Rozanov, C. Schnadt-Poberaj, P. Kenzelmann, A. Fischer, V. Zubov, B. P. Luo, C. Hoyle, T. Egorova, S. Fueglistaler, S. Brönnimann, W. Schmutz and T. Peter, *Atmos. Chem. Phys.*, **8**, 5957–5974, doi:10.5194/acp-8-5957-2008, 2008.
61. T. Egorova, E. Rozanov, V. Zubov, E. Manzini, W. Schmutz and T. Peter, *Atmos. Chem. Phys.*, 2005, **5**, 1557–1576.
62. G. Pitari, E. Mancini, V. Rizi and D. T. Shindell, *J. Atmos. Sci.*, 2002, **59**.
63. J. Austin and N. Butchart, *Q. J. R. Meteorol. Soc.*, 2003, **129**, 3225–3249.
64. W. Tian and M. P. Chipperfield, *Q. J. R. Meteor. Soc.*, 2005, **131**, 281–303.
65. W. Tian M. P. Chipperfield, L. J. Gray and J. M. Zawodny, *J. Geophys. Res.*, **111**, D20301, doi:10.1029/2005JD006871, 2006.
66. O. Morgenstern, P. Braesicke, M. M. Hurwitz, F. M. O'Connor, A. C. Bushell, C. E. Johnson and J. A. Pyle, *Geophys. Res. Lett.*, **35**, L16811, doi:10.1029/2008GL034590, 2008.
67. O. Morgenstern, P. Braesicke, F. M. O'Connor, A. C. Bushell, C. E. Johnson, S. M. Osprey and J. A. Pyle, *Geosci. Model Dev.*, 2009, **1**, 43–57.
68. R. R. Garcia, D. R. Marsh, D. E. Kinnison, B. A. Boville and F. Sassi, *J. Geophys. Res.*, **112**, D09301, doi:10.1029/2006JD007485, 2007.